Orthonormal Vector Polynomials in a Unit Circle, Application: Fitting mapping distortions in a null test

Chunyu Zhao and James H. Burge
College of optical Sciences
The University of Arizona
1630 E. University Blvd.
Tucson, AZ 85721

ABSTRACT

We developed a complete and orthonormal set of vector polynomials defined over a unit circle. One application of these vector polynomials is for fitting the mapping distortions in an interferometric null test. This paper discusses the source of the mapping distortions and the approach of fitting the mapping relations, and justifies why the set of vector polynomials is the appropriate choice for this purpose. Examples are given to show the excellent fitting results with the polynomials.

Keywords: mapping distortion, optical testing, aberration

1. INTRODUCTION

Interferometric testing of steep aspheric surfaces typically uses a null lens, which is designed to transform the spherical wavefront from the interferometer into an aspheric wavefront matching the optic under test. The null lens also images the test optic to an intermediate image which is then relayed to the camera by the interferometer optics. Due to the lack of design degree of freedom, the imaging property of the null lens is usually accepted as a necessary consequence of the required wavefront correction. As a result, the null lens has imaging aberrations, predominantly the mapping distortion. Thus the image of the optic under test will suffer nonlinear mapping onto the sensor.[1-2] It is necessary to correct the mapping distortion to obtain the faithful surface map of the test optic, especially when removing alignment effects, such as tilt, or when the measurement is used to guide figuring of the optic. The analysis of mapping distortion and the optimal definition using the orthonormal vector basis is treated in this paper.

The mapping distortion is quantified using a mapping relation that transforms the undistorted, true physical coordinates at the mirror to the distorted coordinates in data space.,

$$\vec{r}_{distorted} = \mathrm{M}(\vec{r}_{un-distorted}) \tag{1}$$

where $\vec{r}_{distorted}$ is a point in the measurement map in units of pixels and $\vec{r}_{un-distorted}$ is a point on the test optic surface in physical units such as millimeters. A common method for measuring this mapping uses fiducials on the test optic such that their positions, $\vec{r}_{un-distorted}$, are known. Then locate their images $\vec{r}_{distorted}$ in the distorted measurement map.[3-5] Figure 2 shows the pictures of the fiducial masks on the test optic and its image on the detector inside the interferometer. The mapping relation M can be fitted with the known set of $\vec{r}_{un-distorted}$ and $\vec{r}_{distorted}$. With this mapping relation known, any point of the test optic can find its matching point in the distorted measurement map, thus a faithful, undistorted map can be created where interpolation is nearly always necessary.

czhao@optics.arizona.edu ; phone 520-626-6826, fax 520-621-3389

Optical Manufacturing and Testing VIII, edited by James H. Burge, Oliver W. Fähnle, Ray Williamson,
Proc. of SPIE Vol. 7426, 74260V · © 2009 SPIE · CCC code: 0277-786X/09/$18 · doi: 10.1117/12.828288

In previous papers[6-7], we developed a complete and orthonormal set of vector polynomials defined over a unit circle. The set consists of two subsets – one is called S polynomials and the other T polynomials. The S subset has 0 curl and the T subset has 0 divergence. And both S and T vector polynomials are expressed as the linear combinations of standard Zernike polynomials. This set of polynomials is the natural choice for fitting the mapping relations between the test optic and its distorted image, which actually provided the motivation to develop the basis in the first place.

This paper shows how to apply the orthonormal vector basis to the problem of nonlinear mapping in optical testing. More details of the analysis behind this method are provided in a companion paper.[8] In Section 2, we analyze the fundamental cause of the distortion. Based on that, we justify why the polynomials are the appropriate choice for fitting the mapping distortion. In Section 3, we show some of the low order S and T polynomials plots. It is obvious the basic mapping relations are the lowest order of the polynomials. In Section 4, we show how the rotation can be linearly fitted with combinations of S and T polynomials. We presented an example in Section 5 to show the excellent fitting result with these polynomials.

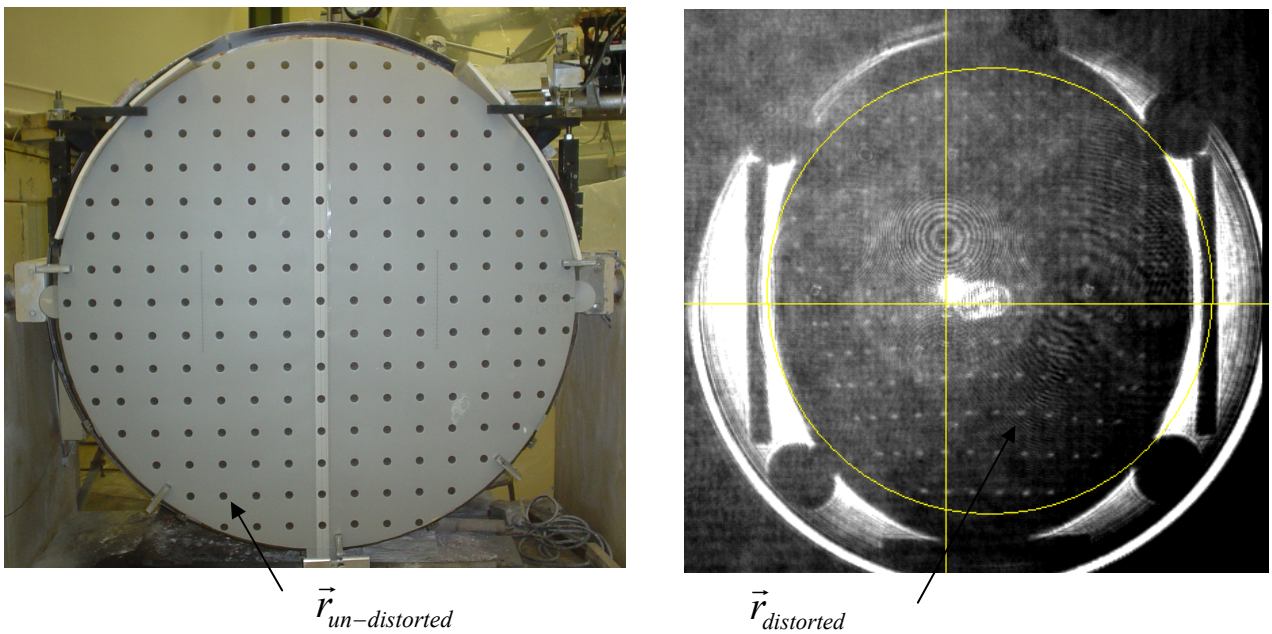

Figure 1. Fiducial masks are used to get the matching points from the test optic and its distorted image. The bright spots in the right picture are images of the holes in the screen shown in the left picture. The coordinate of these points are then used to fit the mapping relations.

2. ORIGIN OF MAPPING DISTORTION

Figure 2 shows a null test for a 1.7m diameter off-axis parabola. The null lens is composed of a 0.5m diameter fold sphere and a CGH. The full aperture interferogram is egg-shaped due to the mapping distortions. And the shape looks like the beam footprint at the CGH. The beam footprint can be thought of as the ray aberrations at the plane of the CGH. As we know, the ray aberrations are proportional to the slopes of the wavefront aberration. In many cases, the wavefront can be well described by Zernike polynomials, the mapping distortion can therefore be well described by Zernike gradient. Since the S polynomials are sum of Zernike gradients, they make an excellent candidate set of polynomials for fitting the mapping distortion in a null test.

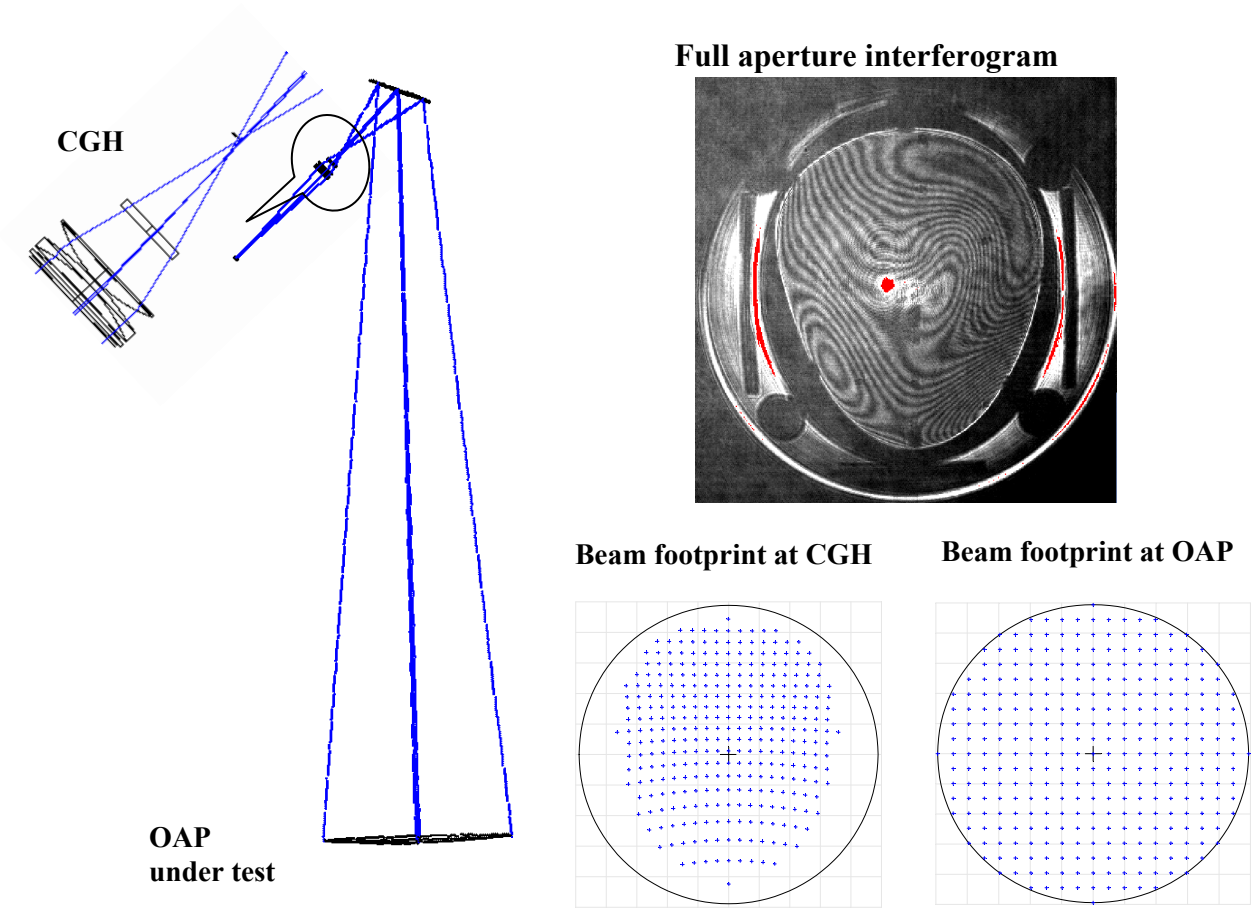

Figure 2. Schematic of the null test of a 1.7m diameter off-axis parabola where the null lens consists of a 0.5m diameter fold sphere and a CGH. The full aperture interferogram manifests the mapping distortion in the test.

3. FITTING MAPPING DISTORTIONS WITH THE S AND T VECTOR POLYNOMIALS

The S and T vector polynomials have the following characteristics:

1. Defined as continuous functions over unit circle
2. Orthonormal, meaning that they are all linearly independent and each has unit magnitude
3. S has 0 curl and can be written as sum of Zernike gradients
4. T has 0 divergence
5. Each T term is a 90 degree rotation of a corresponding S term

Some low order S and T terms are plotted in Figure 3 and 4, respectively.

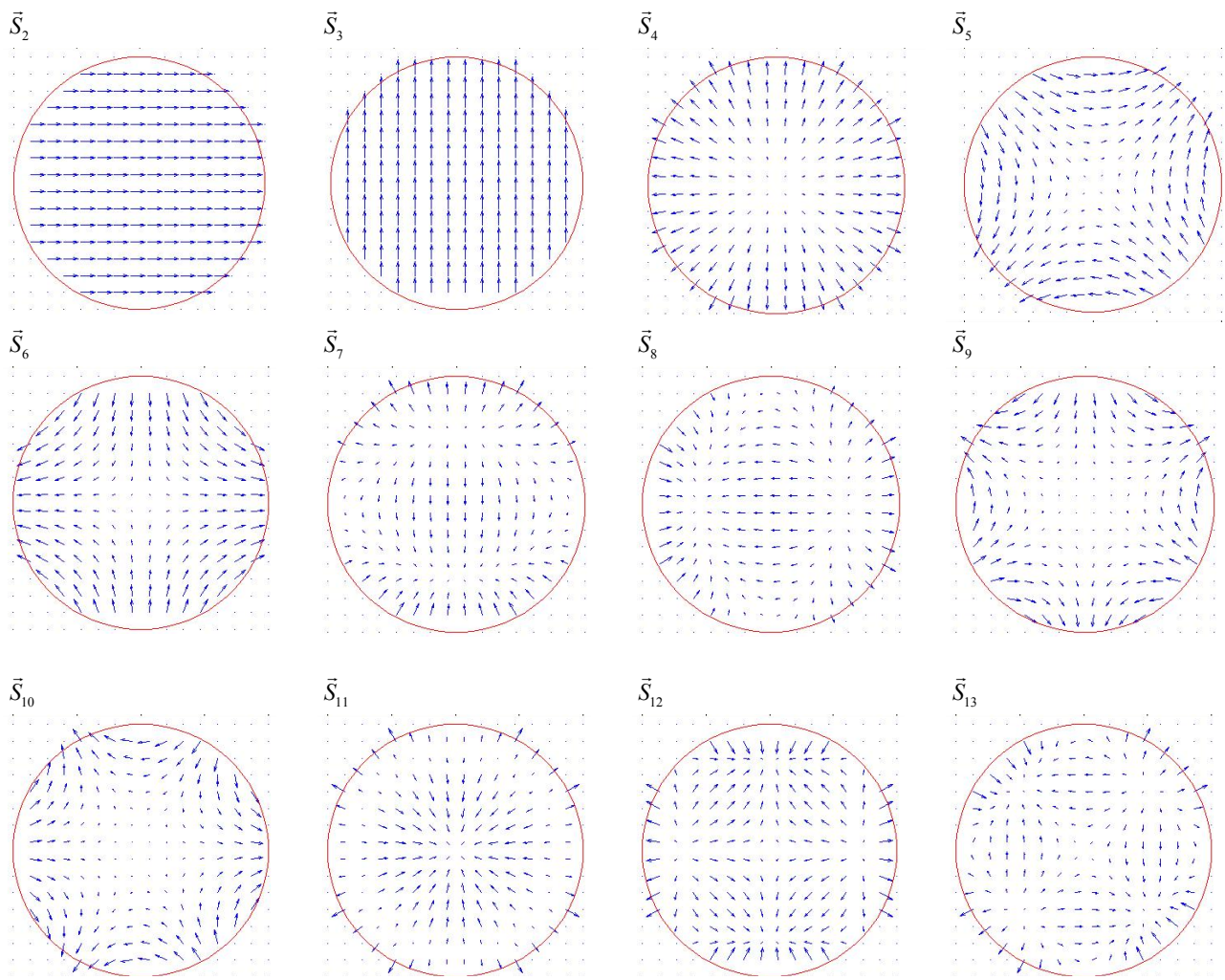

Figure 3. Plots of some low order S terms.

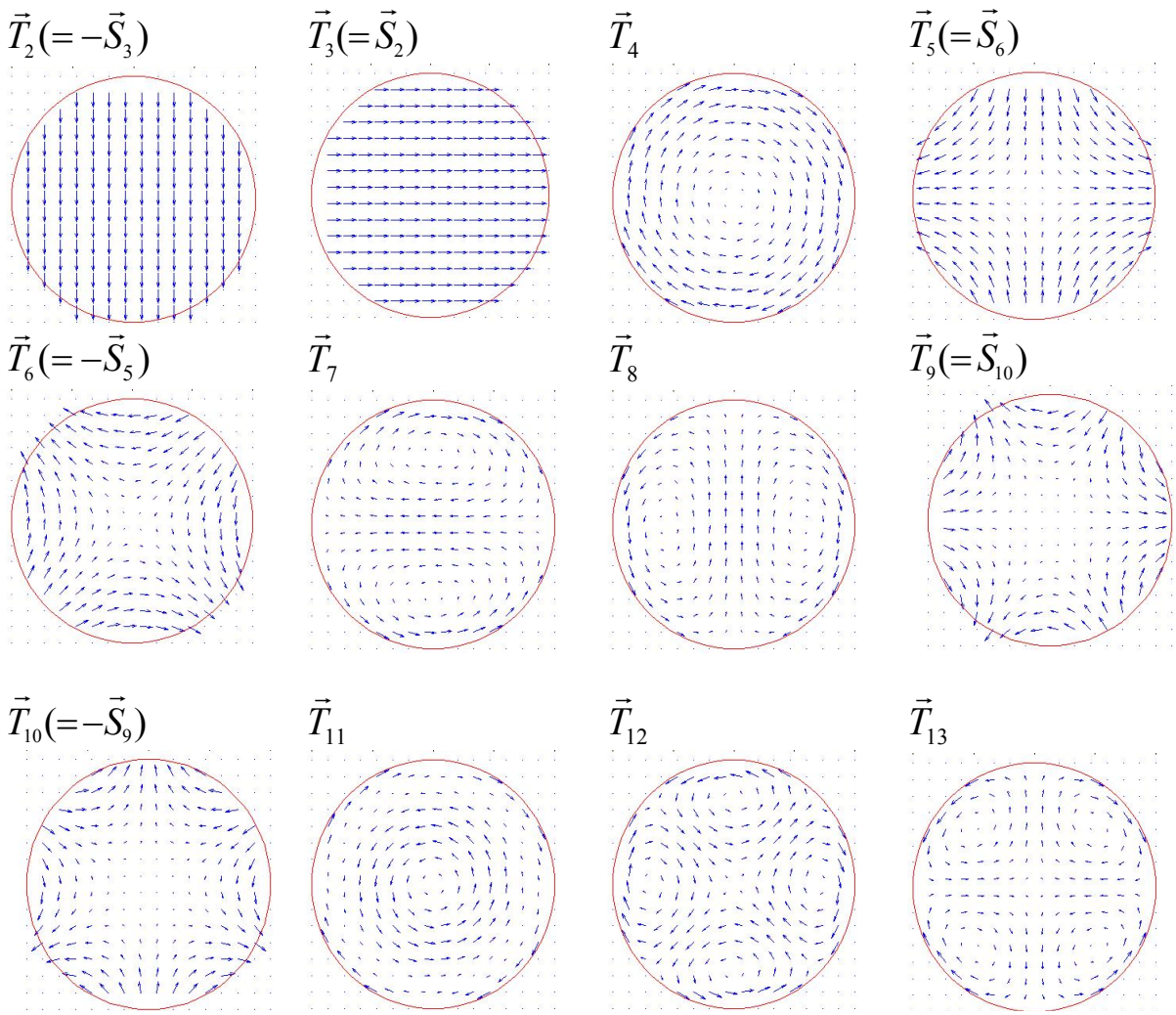

Figure 4. Plots of some low order T terms.

The S2 and S3 functions represent translations in x and y. The S4 function represents scaling. And S5 and S6 represent anamorphism along 45° and 0°, respectively. The T4 function may seem like a fundamental rotation mode, but it is not. T4 represents clockwise rotation followed by scale of √2. Yet it is not scalable, i.e. we can get an infinitesimal rotation from T4, but we can not scale this to get an arbitrary rotation.

$$\vec{T}_4 = \frac{1}{\sqrt{2}}(\hat{i}y - \hat{j}x)$$

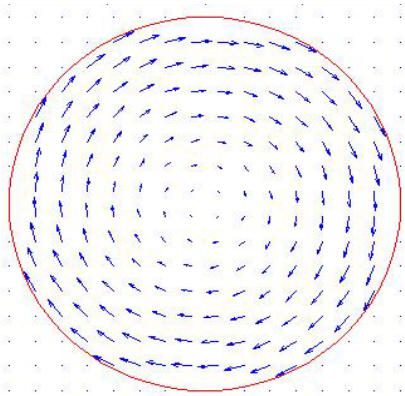

Figure 5. Plot of T4. It looks like the rotation mode, but it is only valid for an infinitesimal rotation. A finite rotation cannot be made by scaling any linear mapping relation, and must be described with either a coordinate transformation or using additional terms. .

4. FITTING ROTATION

As the rays propagate, there is no mechanism for them to twist to produce a rotation. So we conclude that the inherent mapping distortion comes solely from the wavefront distortion and the rotation just comes from choice of coordinate system. Therefore, the distortion can be fully described by the S polynomials. With introduction of T polynomials, the basis is complete and mapping distortion coupled with rotation can be fit linearly.

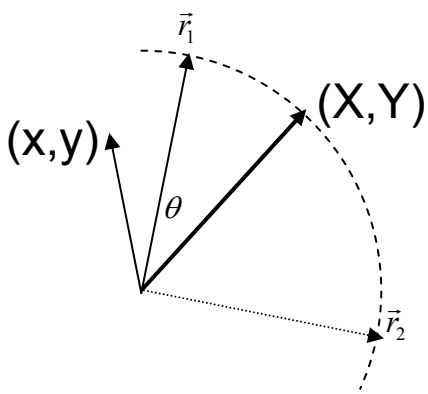

Figure 6. Illustration of mapping form a point (x, y) at the test optic to a point (X, Y) at the image plane. The mapping distortions consist of the inherent distortion caused by wavefront distortion coupled with rotation which is due to choice of the coordinate system.

Figure 6 illustrates the inherent mapping distortions coupled with rotation. The distortion fitting can be divided into two steps:

1. (x,y) to $\vec{r}_1$, which can be fitted with S only.
2. $\vec{r}_1$ rotates θ angle to (X, Y).

To fit the mapping in one step, we introduce another vector $\vec{r}_2$, which is 90° rotation of $\vec{r}_1$. With

$$\vec{r}_1 = \sum a_i \vec{S}_i(x, y), \tag{2}$$

we obtain

$$\vec{r}_2 = \sum a_i \vec{T}_i(x, y), \tag{3}$$

such that

$$(X, Y) = \cos\theta \cdot \vec{r}_1 + \sin\theta \cdot \vec{r}_2 = \sum (A_i \vec{S}_i(x, y) + B_i \vec{T}_i(x, y)). \tag{4}$$

Eq. (4) shows that the mapping distortion coupled with rotation can be linearly fitted with combinations of S and T terms.

5. AN EXAMPLE

The off-axis parabola shown in Figure 1 was later tested with a single CGH where the mapping distortion is even worse. Figure 7 shows the beam footprint diagrams at both the CGH and the test surface, and the distorted measurement map and the morphed surface map. Note that again the beam footprint at the CGH resembles the actual shape of the measurement map. After the mapping relation is fitted, a distortion corrected map is generated as shown in Figure 7d where the fiducials are back to the regular grid positions.

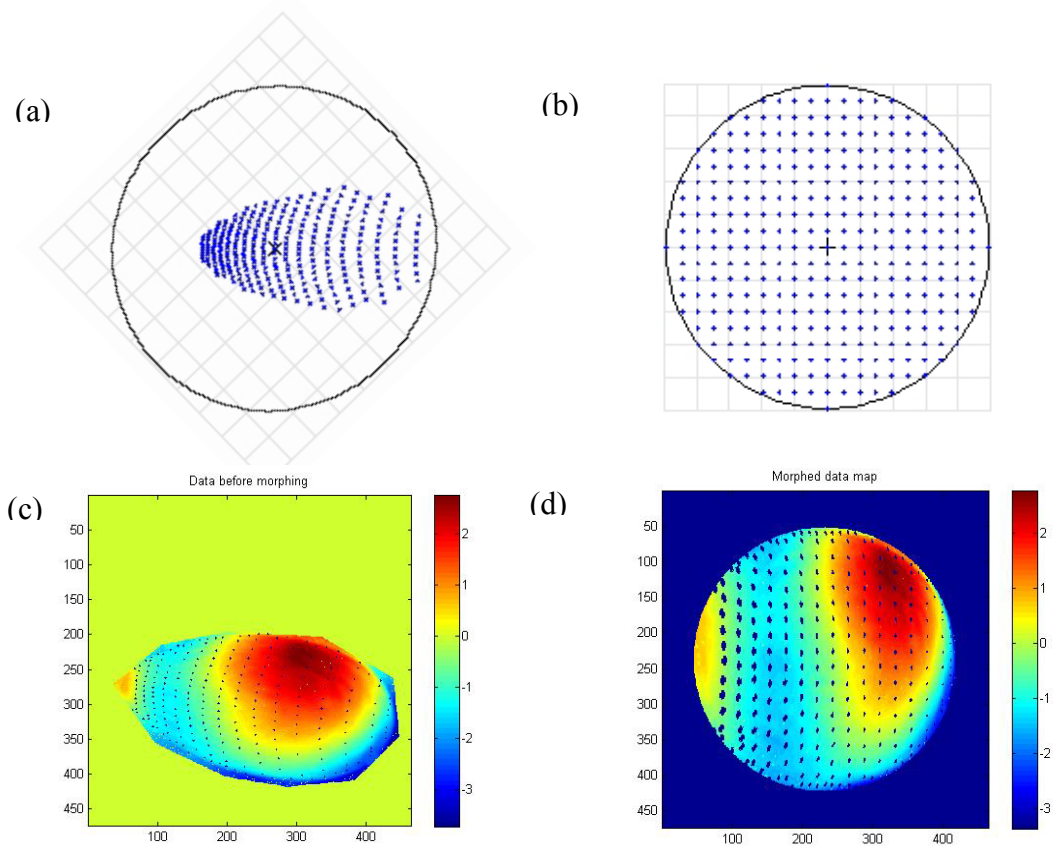

Figure 7. the beam footprint diagram at (a) the CGH, and (b) the test off-axis parabola surface. (c) the measurement map with fiducial images, and (d) the distortion corrected surface map.

6. SUMMARY

In this paper, we analyze the root cause of the mapping distortion in an interferometric null test of an aspheric surface and propose to fit the mapping distortion with a set of vector polynomials defined over a unit circle. A system designed for testing an off-axis parabola, where substantial amount of mapping distortion is present, was studied. The vector polynomials are used to fit the mapping distortion and excellent result was achieved.

REFERENCES

[1] F. Schillke, "Critical aspects on testing aspheres in interferometric setups," Proc. SPIE **3739**, 317–324 (1999).

[2] S. Reichelt, C. Pruss, and H. J. Tiziani, "New design techniques and calibration methods for CGH-null testing of aspheric surfaces," Proc. SPIE **4778**, 158–168 (2002).

[3] J. E. Hayden and T. S. Lewis, "Distortion correction method for aspheric optical testing," Proc. SPIE **4101**, 57–63 (2000).

[4] C. Zhao, R. A. Sprowl, M. Bray, and J. H. Burge, "Figure measurement of a large optical flat with a Fizeau interferometer and stitching technique," Proc. SPIE **6293**, 62930K (2006).

[5] B. M. Robinson and P. J. Reardon, "Distortion compensation in interferometric testing of mirrors," Appl. Opt. **48**, 560-565 (2009)

[6] C. Zhao and J. H. Burge, "Orthonormal vector polynomials in a unit circle, Part I: basis set derived from gradients of Zernike polynomials," Opt. Express **15**, 18014-18024 (2007)

[7] C. Zhao and J. H. Burge, "Orthonormal vector polynomials in a unit circle, Part II : completing the basis set," Opt. Express **16**, 6586-6591 (2008).

[8] C. Zhao and J. H. Burge, "Use of orthonormal vector polynomials to define mapping distortion for optical testing," submitted to Opt. Express (2009)